

Ab Initio Many-Body Calculations of n - ^3H , n - ^4He , p - $^3,^4\text{He}$, and n - ^{10}Be Scattering

Sofia Quaglioni* and Petr Navrátil⁺

Lawrence Livermore National Laboratory, P.O. Box 808, L-414, Livermore, California 94551, USA

(Received 15 April 2008; published 29 August 2008)

We develop a new *ab initio* many-body approach capable of describing simultaneously both bound and scattering states in light nuclei, by combining the resonating-group method with the use of realistic interactions, and a microscopic and consistent description of the nucleon clusters. This approach preserves translational symmetry and Pauli principle. We present phase shifts for neutron scattering on ^3H , ^4He , and ^{10}Be and proton scattering on $^3,^4\text{He}$, using realistic nucleon-nucleon potentials. Our $A = 4$ scattering results are compared to earlier *ab initio* calculations. We demonstrate that a proper treatment of the coupling to the n - ^{10}Be continuum is successful in explaining the parity-inverted ground state in ^{11}Be .

DOI: 10.1103/PhysRevLett.101.092501

PACS numbers: 21.60.De, 25.10.+s, 27.10.+h, 27.20.+n

The development of an *ab initio* theory of low-energy reactions on light nuclei is key to further refining our understanding of the fundamental internucleon interactions and providing accurate predictions of crucial reaction rates for nuclear astrophysics. However, *ab initio* calculations for scattering processes involving more than four nucleons overall are challenging and still a rare exception [1]. In this Letter, we combine the resonating-group method (RGM) [2] and the *ab initio* no-core shell model (NCSM) [3] into a new many-body approach (*ab initio* NCSM/RGM) capable of treating bound and scattering states of light nuclei in a unified formalism. The RGM is a microscopic cluster technique based on A -nucleon Hamiltonians, using fully antisymmetric many-body wave functions built assuming that the nucleons are grouped into clusters. The NCSM is an *ab initio* approach to the microscopic calculation of ground and low-lying excited states of light nuclei with realistic two- (NN) and, in general, three-nucleon (NNN) forces. Here, we complement the ability of the RGM to deal with scattering and reactions with the use of realistic interactions and a consistent *ab initio* description of the nucleon clusters, achieved via the NCSM. Within this new approach, we study the n - ^3H , n - ^4He , n - ^{10}Be , and p - $^3,^4\text{He}$ scattering processes and address the parity inversion of the ^{11}Be ground state (g.s.), using realistic NN potentials.

We start from the wave function for a scattering process involving pairs of nuclei that can be cast in the form

$$|\Psi^{J\pi T}\rangle = \sum_{\nu} \int dr r^2 \frac{g_{\nu}^{J\pi T}(r)}{r} \hat{\mathcal{A}}_{\nu} |\Phi_{\nu r}^{J\pi T}\rangle, \quad (1)$$

through an expansion over binary-cluster channel-states of total angular momentum J , parity π , and isospin T ,

$$|\Phi_{\nu r}^{J\pi T}\rangle = [(|A-a \alpha_1 I_1^{\pi_1} T_1\rangle |a \alpha_2 I_2^{\pi_2} T_2\rangle)^{(ST)} Y_{\ell}(\hat{r}_{A-a,a})]^{(J\pi T)} \times \frac{\delta(r - r_{A-a,a})}{r r_{A-a,a}}. \quad (2)$$

The wave functions of the $(A-a)$ - and a -nucleon clusters are each antisymmetric and depend on translationally in-

variant internal coordinates. They are eigenstates of the $H_{(A-a)}$ and $H_{(a)}$ intrinsic Hamiltonians with spin, parity, isospin, and additional quantum numbers I_i , π_i , T_i , and α_i , respectively, where $i = 1, 2$. The centers of mass of the two clusters are separated by the relative vector $\vec{r}_{A-a,a}$. Relative angular momentum and channel spin are denoted by ℓ and s , respectively. The intercluster antisymmetrizer for the $(A-a, a)$ partition in Eq. (1) can be schematically written as $\hat{\mathcal{A}}_{\nu} = [(A-a)!a!/A!]^{1/2} \sum_p (-1)^p P$, where P are permutations among nucleons pertaining to different clusters and p the number of interchanges characterizing them. The coefficients of the expansion with respect to the channel index $\nu = \{A-a \alpha_1 I_1^{\pi_1} T_1; a \alpha_2 I_2^{\pi_2} T_2; s\ell\}$ are the relative-motion wave functions $g_{\nu}^{J\pi T}(r)$, which represent the unknowns of the problem. They can be determined by solving the many-body Schrödinger equation in the Hilbert space spanned by the basis states $\hat{\mathcal{A}}_{\nu} |\Phi_{\nu r}^{J\pi T}\rangle$,

$$\sum_{\nu} \int dr r \mathcal{K}_{\nu\nu'}^{J\pi T}(r', r) g_{\nu'}^{J\pi T}(r) = 0, \quad (3)$$

where the integral kernel, nonlocal due to the intercluster antisymmetrizers, is given by

$$\mathcal{K}_{\nu\nu'}^{J\pi T}(r', r) = \langle \Phi_{\nu' r'}^{J\pi T} | \hat{\mathcal{A}}_{\nu'} (H - E) \hat{\mathcal{A}}_{\nu} | \Phi_{\nu r}^{J\pi T} \rangle. \quad (4)$$

Here, E is the total energy in the center-of-mass (c.m.) frame, and H is the intrinsic A -nucleon microscopic Hamiltonian, which it is useful to decompose into, e.g.,

$$H = T_{\text{rel}}(r) + \mathcal{V}_{\text{rel}} + \bar{V}_C(r) + H_{(A-a)} + H_{(a)}. \quad (5)$$

Further, $T_{\text{rel}}(r)$ is the relative kinetic energy, and \mathcal{V}_{rel} is the sum of all interactions between nucleons belonging to different clusters after subtraction of the average Coulomb interaction between them, explicitly singled out in the term $\bar{V}_C(r) = Z_{1\nu} Z_{2\nu} e^2 / r$, where $Z_{1\nu}$ and $Z_{2\nu}$ are the charge numbers of the clusters in channel ν .

We obtain the cluster eigenstates entering Eq. (2) by diagonalizing $H_{(A-a)}$ and $H_{(a)}$ in the model space spanned by the NCSM basis. This is a complete harmonic oscillator

TABLE I. Calculated ${}^3\text{H}$ and ${}^4\text{He}$ g.s. energies (in MeV), n - ${}^3\text{H}$, n - ${}^4\text{He}$, and p - ${}^4\text{He}$ phase shifts (in degrees), and n - ${}^3\text{H}$ and n - ${}^4\text{He}$ total cross sections (in barns) for increasing N_{max} at $\hbar\Omega = 18$ MeV, obtained using the $V_{\text{low}k}$ NN potential (derived from AV18 with cutoff $\Lambda = 2.1$ fm $^{-1}$) [8]. Only the g.s. of the ${}^3\text{H}$ and ${}^4\text{He}$ nuclei were included in the scattering calculations.

${}^3\text{H}$		n - ${}^3\text{H}$ ($E_{\text{kin}} = 0.75$ MeV)							σ_t
N_{max}	$E_{\text{g.s.}}$	0^+ (1S_0)	0^- (3P_0)	1^+ (3S_1)	1^- (1P_1)	1^- (3P_1)	1^- (ϵ)	2^- (3P_2)	
9	-7.80	-27.8	2.30	-26.2	2.19	4.96	-17.5	7.51	1.06
11	-7.96	-31.3	2.39	-28.1	2.63	5.93	-12.7	6.42	1.20
13	-8.02	-32.4	2.15	-28.8	3.10	6.17	-9.1	5.75	1.25
15	-8.11	-33.2	2.45	-29.9	3.46	6.12	-9.5	6.08	1.33
17	-8.12	-34.2	2.60	-30.9	3.74	6.30	-10.7	6.19	1.41
19	-8.16	-34.8	2.49	-31.3	4.00	6.49	-10.1	6.02	1.44

${}^4\text{He}$		n - ${}^4\text{He}$ ($E_{\text{kin}} = 5.0$ MeV)			p - ${}^4\text{He}$ ($E_{\text{kin}} = 5.0$ MeV)			
N_{max}	$E_{\text{g.s.}}$	$\frac{1}{2}^+$ (${}^2S_{1/2}$)	$\frac{1}{2}^-$ (${}^2P_{1/2}$)	$\frac{3}{2}^-$ (${}^2P_{3/2}$)	σ_t	$\frac{1}{2}^+$ (${}^2S_{1/2}$)	$\frac{1}{2}^-$ (${}^2P_{1/2}$)	$\frac{3}{2}^-$ (${}^2P_{3/2}$)
9	-27.00	-57.9	33.5	81.8	1.95	-45.8	31.3	76.5
11	-27.41	-58.6	33.7	86.1	1.98	-46.4	31.9	80.2
13	-27.57	-58.7	34.0	85.7	1.98	-46.6	32.0	80.0
15	-27.75	-58.7	33.9	84.6	1.97	-46.6	32.1	79.9
17	-27.77	-58.6	33.9	84.8	1.97	-46.5	32.0	79.9

(HO) basis, the size of which is defined by the maximum number, N_{max} , of HO quanta above the lowest configuration shared by the nucleons. Thanks to the unique properties of the HO basis, we can use Jacobi-coordinate wave functions [4] for both nuclei or only for the lightest of the pair (typically $a \leq 4$), and still preserve translational invariance. In the second case, we expand the heavier cluster on a Slater-determinant (SD) basis, and remove completely the spurious c.m. components in a similar fashion as in Refs. [5,6]. We exploited this dual approach to verify our results. The use of the SD basis is computationally advantageous and allows us to explore reactions involving p -shell nuclei. In calculating (4), all “direct” terms arising from the identical permutations in both $\hat{\mathcal{A}}_{\nu}$ and $\hat{\mathcal{A}}_{\nu'}$ are treated exactly with the exception of $\langle \Phi_{\nu'\nu'}^{J^{\pi T}} | \mathcal{V}_{\text{rel}} | \Phi_{\nu\nu}^{J^{\pi T}} \rangle$. The latter and all remaining terms are obtained by expanding the Dirac δ of Eq. (2) on a set of HO radial wave functions with identical frequency Ω , and model-space size N_{max} consistent with those used for the two clusters. In this respect, we note that \mathcal{V}_{rel} is localized also in the presence of the Coulomb force. We solve Eq. (3) via the coupled-channel R -matrix method on a Lagrange mesh [7] imposing either bound-state or scattering boundary conditions for $g_{\nu\nu}^{J^{\pi T}}(r)$ at large r .

All calculations in the present Letter were carried out using binary-cluster channels (2) with $a = 1$. We first discuss results obtained expanding the wave function (1) on all the allowed basis states with the $(A - 1)$ -nucleon cluster in its g.s. Table I shows the behavior with respect to N_{max} of selected $A = 4, 5$ data obtained using the $V_{\text{low}k}$ NN potential [8]. The overall convergence is fairly satisfactory, with somewhat larger relative differences for the phase shifts of small magnitude.

In what follows, we present results obtained using effective interactions derived from the underlying realistic NN potential, V_N , through a unitary transformation. Starting from the relevant two-nucleon Hamiltonian (for notation and definitions see Ref. [4]) $H_2^{\Omega} = H_{02} + V_{12}$, with $V_{12} = V_N(\sqrt{2}\tilde{r}) - m\Omega^2\tilde{r}^2/A$, the cluster eigenstates are obtained employing the usual NCSM two-body effective interaction $V_{2\text{eff}} = \hat{H}_{2\text{eff}} - H_{02}$, where $\hat{H}_{2\text{eff}}$ is the Hermitian effective Hamiltonian. However, in place of

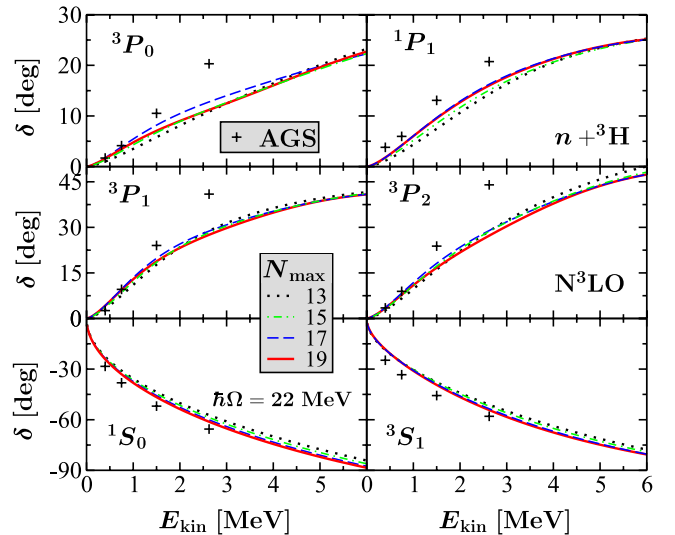
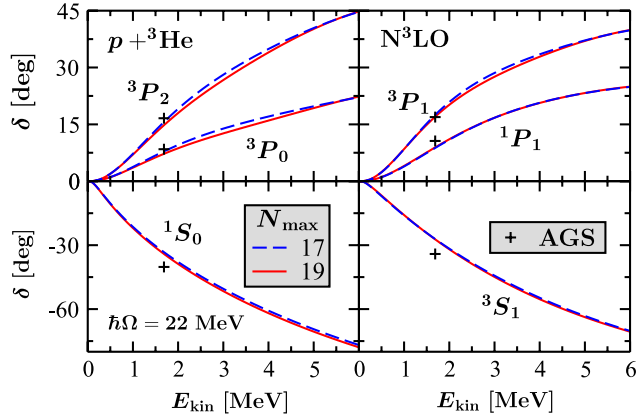
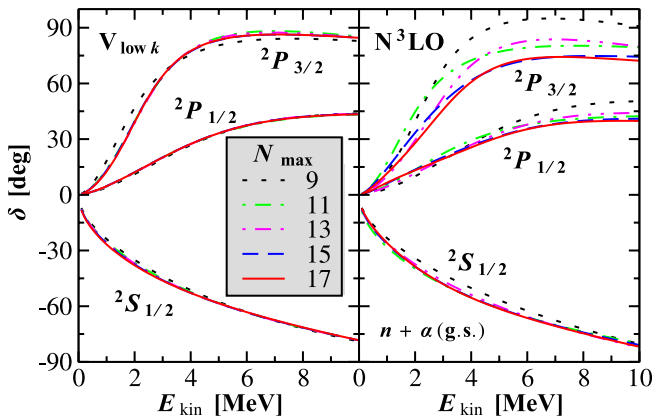
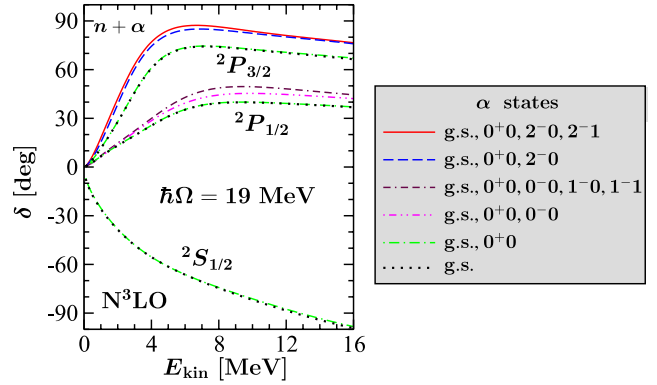


FIG. 1 (color online). Calculated n - ${}^3\text{H}$ phase shifts as a function of the relative kinetic energy in the c.m. frame E_{kin} , using the $N^3\text{LO}$ NN potential [9]. Only the $(A - 1)$ -cluster g.s. were included in the present calculation. Dependence on N_{max} at $\hbar\Omega = 22$ MeV compared to AGS results of Ref. [10,11].

FIG. 2 (color online). Same as Fig. 1 for p - ${}^3\text{He}$ scattering.

the bare NN potential entering \mathcal{V}_{rel} , we adopted the new effective interaction $V'_{2\text{eff}} = \bar{H}_{2\text{eff}} - \bar{H}'_{2\text{eff}}$, where $\bar{H}'_{2\text{eff}}$ is the effective Hamiltonian derived from $H_2^{\Omega'} = H_{02} + V'_{12}$, with $V'_{12} = -m\Omega^2 \tilde{r}^2/A$. Note that $V'_{2\text{eff}} \rightarrow V_N$ in the limit $N_{\text{max}} \rightarrow \infty$. Figures 1 and 2 and the right panel of Fig. 3 present $A = 4, 5$ scattering phase shifts for the $N^3\text{LO}$ NN potential [9] derived within chiral effective-field theory at next-to-next-to-next-to-leading order. For the whole energy range, we find less than 2 deg absolute difference between the phases obtained in the largest and next-to-largest model spaces, a sign of convergence. The only exception is represented by the ${}^2P_{3/2}$ phase shifts of the n - α system, for which this difference rises up to 5 deg in the range $1 \text{ MeV} < E_{\text{kin}} < 4 \text{ MeV}$. As a comparison, we show in the left panel of Fig. 3 the n - α phase shifts obtained with the (bare) $V_{\text{low}k}$ interaction. The convergence rate is clearly much faster for $V_{\text{low}k}$.

To verify our approach, in Figs. 1 and 2, we compare our n - ${}^3\text{H}$ and p - ${}^3\text{He}$ results to earlier *ab initio* calculations performed within the Alt, Grassberger, and Sandhas (AGS) formalism [10,11], using the same $N^3\text{LO}$ NN po-

FIG. 3 (color online). Dependence on N_{max} of the n - α (g.s.) phase shifts with the $V_{\text{low}k}$ [8] (left panel) and $N^3\text{LO}$ [9] (right panel) NN potentials at $\hbar\Omega = 18$ and 19 MeV , respectively.FIG. 4 (color online). Influence of the lowest six excited states (0^+0 , 0^-0 , 1^-0 , 1^-1 , 2^-0 , 2^-1) of the α particle on the n - α phase-shift results for the $N^3\text{LO}$ NN potential [9].

tential. In general, the agreement between the two calculations worsens as the relative kinetic energy in the c.m. frame, E_{kin} , increases. For the P -waves, in particular, we can reasonably reproduce the AGS calculation within 1 MeV off threshold, while we can find differences as large as 17 deg (3P_2) at $E_{\text{kin}} = 2.6 \text{ MeV}$. These discrepancies are due to the influence played by closed channels not included in our calculations, such as those with the $A - 1 = 3$ eigenstates above the $I_1^{\pi_1} = \frac{1}{2}^+$ g.s., and $(A - a = 2, a = 2)$ configurations, present in the AGS results. In Ref. [10], it was shown that the omission of three-nucleon partial waves with $\frac{1}{2} < I_1 \leq \frac{5}{2}$ leads to comparable effects.

We explore the effect of the inclusion of excited states of the $(A - 1)$ -cluster on the $A = 5$ system. Channels with $a > 1$ have here a much suppressed effect due to the large binding energy of the ${}^4\text{He}$ nucleus. Figure 4 shows n - α phase shifts for six sets of binary-cluster channels obtained including the six combinations of ${}^4\text{He}$ states listed in the legend. The ${}^2S_{1/2}$ phase shifts are affected minimally by

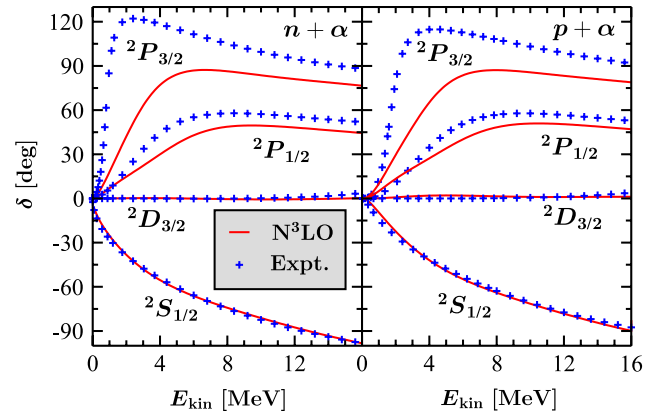
FIG. 5 (color online). Calculated n - α (left panel) and p - α (right panel) phase shifts for the $N^3\text{LO}$ NN potential [9], including the ${}^4\text{He}$ g.s., 0^+0 , 0^-0 , 1^-0 , 1^-1 , 2^-0 , and 2^-1 states, compared to an R -matrix analysis of data (+) [12].

TABLE II. Calculated energies (in MeV) of the ^{10}Be g.s. and of the lowest negative- and positive-parity states in ^{11}Be , obtained using the CD-Bonn NN potential [13] at $\hbar\Omega = 13$ MeV. The NCSM/RGM results were obtained using $n + ^{10}\text{Be}$ configurations with $N_{\text{max}} = 6$ g.s., 2_1^+ , 2_2^+ , and 1_1^+ states of ^{10}Be .

	N_{max}	^{10}Be		$^{11}\text{Be}(\frac{1}{2}^-)$		$^{11}\text{Be}(\frac{1}{2}^+)$	
		$E_{\text{g.s.}}$	E	E_{th}	E	E_{th}	E
NCSM [14,15]	8/9	-57.06	-56.95	0.11	-54.26	2.80	
NCSM [14,15] ^a	6/7	-57.17	-57.51	-0.34	-54.39	2.78	
NCSM/RGM ^a			-57.59	-0.42	-57.85	-0.68	
E _{xpt.}		-64.98	-65.16	-0.18	-65.48	-0.50	

^apresent calculation.

the 0^+0 excited state, while no further corrections are found in the four larger Hilbert spaces (the $^2S_{1/2}$ results of which we omit for clarity of the figure). We find larger deviations on the $^2P_{1/2}$ and $^2P_{3/2}$ phase shifts, after inclusion of the 0^-0 , 1^-0 , and 1^-1 states for the first, and of the 2^-0 and 2^-1 states for the second.

In Fig. 5, the n - and p - α phase shifts obtained with the $N^3\text{LO}$ NN potential, including the first six ^4He excited states, are compared to an accurate multichannel R -matrix analysis of the nucleon- α scattering data [12]. The $^2S_{1/2}$ phase shifts are in good agreement with experiment, also in the presence of the p - α Coulomb repulsion. The magnitude of the $^2D_{3/2}$ phase shifts is also qualitatively reproduced. On the contrary, the P phase shifts present both insufficient magnitude and splitting with respect to the R -matrix analysis. The $\frac{1}{2}^+$ channel is dominated by the repulsion between nucleon and α particle induced by the Pauli exclusion principle. Consequently, the short-range details of the nuclear interaction play a minor role on the $^2S_{1/2}$ phase shifts, for which, as shown in Fig. 3, we find very similar results using the $V_{\text{low}k}$ potential. On the other hand, the $^2P_{1/2}$ and $^2P_{3/2}$ phase shifts show sensitivity to the interaction model, and, in particular, to the strength of the spin-orbit force. The present discrepancy with respect to experiment may be due to the omission of the NNN terms of the chiral interaction, which would probably enhance the spin-orbit splitting.

To show the promise and flexibility of our approach, we present in Table II and Fig. 6 results for a much heavier ($A = 11$) system. The parity-inverted g.s. of ^{11}Be , one of the best examples of disappearance of the $N = 8$ magic number with increasing N/Z ratio, has been so far left unexplained by *ab initio* calculations [15]. Possibly the NNN interaction plays a role in the inversion mechanism. In any case, only when an approach is capable of describing the ^{11}Be halo can one obtain a meaningful insight. The HO asymptotic behavior in the standard NCSM does not favor extended n - ^{10}Be configurations [15], thus altering the S -wave relative kinetic and potential energies, with a re-

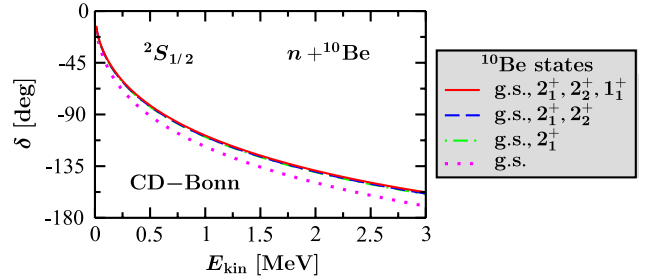


FIG. 6 (color online). Calculated $^2S_{1/2}$ n - ^{10}Be phase shifts as a function of E_{kin} . NCSM/RGM calculation as in Table II. The obtained scattering length is +10.7 fm.

sulting net underbinding of the $^{11}\text{Be} \frac{1}{2}^+$ state. In the *ab initio* NCSM/RGM, one gets the correct relative kinetic energy, due to the rescaling of the relative wave function in the internal region when the Whittaker tail is recovered. This is the main cause of the dramatic decrease (~ 3.5 MeV) of the energy of the $\frac{1}{2}^+$ state, which makes it bound and even leads to a g.s. parity inversion.

We thank A. Deltuva, P. Descouvemont, J. Hale, and I. J. Thompson for valuable discussions. Numerical calculations have been performed at the LLNL LC facilities. Prepared by LLNL under Contract DE-AC52-07NA27344. Support from the U.S. DOE/SC/NP (Work Proposal No. SCW0498), and from the U.S. Department of Energy Grant DE-FC02-07ER41457 is acknowledged.

*quaglioni1@llnl.gov

+navratil1@llnl.gov

- [1] K. M. Nollett *et al.*, Phys. Rev. Lett. **99**, 022502 (2007).
- [2] Y. C. Tang *et al.*, Phys. Rep. **47**, 167 (1978); K. Langanke and H. Friedrich, *Advances in Nuclear Physics*, edited by J. W. Negele and E. Vogt (Plenum, New York, 1986).
- [3] P. Navrátil, J. P. Vary, and B. R. Barrett, Phys. Rev. Lett. **84**, 5728 (2000); Phys. Rev. C **62**, 054311 (2000).
- [4] P. Navrátil, G. P. Kamuntavičius, and B. R. Barrett, Phys. Rev. C **61**, 044001 (2000).
- [5] P. Navrátil, Phys. Rev. C **70**, 014317 (2004).
- [6] P. Navrátil, Phys. Rev. C **70**, 054324 (2004).
- [7] M. Hesse *et al.*, Nucl. Phys. A **640**, 37 (1998); M. Hesse, J. Roland, and D. Baye, Nucl. Phys. A **709**, 184 (2002).
- [8] S. K. Bogner, T. T. S. Kuo, and A. Schwenk, Phys. Rep. **386**, 1 (2003); G. Hagen (private communication).
- [9] D. R. Entem and R. Machleidt, Phys. Rev. C **68**, 041001 (R) (2003).
- [10] A. Deltuva and A. C. Fonseca, Phys. Rev. C **75**, 014005 (2007); Phys. Rev. Lett. **98**, 162502 (2007).
- [11] A. Deltuva (private communication).
- [12] G. M. Hale (private communication).
- [13] R. Machleidt, Phys. Rev. C **63**, 024001 (2001).
- [14] E. Caurier *et al.*, Phys. Rev. C **66**, 024314 (2002).
- [15] C. Forssen *et al.*, Phys. Rev. C **71**, 044312 (2005).